CHEMICAL ENGINEERING RESEARCH AND DESIGN XXX (2013) XXX–XXX

Contents lists available at SciVerse ScienceDirect

Chemical Engineering Research and Design

journal homepage: www.elsevier.com/locate/cherd

Catalytic hydrogen adsorption of nano-crystalline hydrotalcite derived mixed oxides

M. Abdus Salam, Suriati Sufian, T. Murugesan*

Chemical Engineering Department, Universiti Teknologi PETRONAS, Bandar Sri Iskandar, 31750 Tronoh, Perak, Malaysia

ABSTRACT

Nano-crytalline hydrotalcite derived reduced mixed oxides containing magnesium, nickel and aluminium (MNAM) have been synthesized using coprecipitation and showed successfully nickel catalysed reversible hydrogen adsorption using the temperature programmed technique under near ambient conditions. ICP-MS and XRD analysis ensured the adsorbent homogeneity and different crystalline phases of mixed oxides. Morphology and textural properties of mixed oxides have been explored using the FESEM, BET and HRTEM analysis techniques. Nano-crystalline and mesporous reduced mixed oxides exhibited a 3.9 wt% H_2 adsorption capacity in where desorption capacity was 1.9 wt% H_2. Hydrogen adsorbed surface and different phases were analysed by XPS, Raman and FTIR analysis techniques. The hydrogen adsorption enthalpy (ΔH) and entropy (ΔS) changes of reduced mixed oxides were −47.58 kJ/mol and −120.98 J/mol K, respectively, and the promising desorption activation energy of 65 kJ/mol correspond its reversibility as potential energy storage material.

© 2013 The Institution of Chemical Engineers. Published by Elsevier B.V. All rights reserved.

Keywords: Adsorption; Catalytic; Mixed oxides; Thermodynamics; Nano-crystalline

1. Introduction

Hydrogen is a potential energy carrier and one of the emission free future fuels. Nano-crystalline particles enhance hydrogen storage and release kinetics (Cornelis et al., 2006) and often show different behaviour compared to bulk particles. Hydrogen can be stored via physical way such as compressed and liquid hydrogen gas methods, and chemical way via metal hydrides and complex hydrides (Vajo and Olson, 2007). Metal hydrides are potential hydrogen storage material that can meet the demand of on board vehicles as primary energy source. None of them meet the U.S department of energy (DOE) goal yet for reversible hydrogen storage. Magnesium has been explored in different ways due to its high gravimetric and volumetric hydrogen density and its availability (Bogdanovic et al., 1993). Magnesium can form a structure (MgH_2) with 7.6 wt% hydrogen. Nickel can be used as catalyst to dissociate hydrogen and enhance the hydrogen sorption (Borgschulte et al., 2006). When hydrogen combines with magnesium (Mg), it forms the inter-metallic compound. Ternary hydride alloy, Mg_2Ni can form a hydrogen-rich hydride complex such as Mg_2NiH_4. The material which could store hydrogen at near ambient conditions via physical and/or chemical way and release hydrogen at low decomposition temperature might be a promising material for hydrogen storage (Arean et al., 2010). Some materials exhibit high hydrogen storage capacities such as alanates and metal hydrides but their practical use is limited due to their non-favourable thermodynamics and kinetics and their regeneration limitation.

Mixed oxides have recently emerged as promising candidates of hydrogen gas adsorbents. Hydrotalcite derived mixed oxides have important features in forming highly dispersed metallic particles upon reduction (Salam et al., 2013, 2013a, 2013b). Controlled thermal decomposition of hydrotalcites produced high specific surface area of mixed oxides that have various applications such as removal of CO_2, SO_x and NO_x, partial oxidation and hydrogenation (Bergada et al., 2007; Kirm et al., 2004; Mahasweta et al., 2009). Another important property of this material is acid–base pairs that can be created active site for many reaction or gas adsorption. The acid–base properties of hydrotalcite derived mixed oxides are governed by the molar ratios, calcination temperature and synthesis

* *Corresponding author*. Fax: +60 5 365 6176.
E-mail address: salam.bcsir@gmail.com (M.A. Salam).
Received 10 January 2013; Received in revised form 11 May 2013; Accepted 28 May 2013
0263-8762/$ – see front matter © 2013 The Institution of Chemical Engineers. Published by Elsevier B.V. All rights reserved.
http://dx.doi.org/10.1016/j.cherd.2013.05.024

Please cite this article in press as: Salam, M.A., et al., Catalytic hydrogen adsorption of nano-crystalline hydrotalcite derived mixed oxides. Chem. Eng. Res. Des. (2013), http://dx.doi.org/10.1016/j.cherd.2013.05.024

conditions. The surface of the reduced mixed oxides is more reactive than the oxide with the gases and can form possible yields (Shouli et al., 2010). The surface energy and texture of the adsorbents enhance the physical adsorption. Hydrogen gas can react chemically with the basic side of the hydrotalcite derived metal oxides. Mixed oxides have the ability to recover the layered structure after rehydration or immersion in solutions containing anions. Hydrotalcite derived mixed oxides with different cations are well dispersed and interactive showed moderate interaction (Kubas interaction) with hydrogen (Salam et al., 2013a, 2013b). After hydrogen treatment (H_2 reduction), mixed oxides contain anion vacancies generated by the elimination of water (H_2O). The vacancies created on the surface of the solids are able to capture/receive hydrogen in hydride form. Mixed oxides have gained considerable attention in being designed as adsorbent due to their wide variety of chemical compositions (Bergaya et al., 2006) and their textural and surface morphology that can be tuned. Mixed oxides formation leads to the modification of an electronic structure, the band gap, Fermi level position and transport properties etc. in the solid solution (Zakrzewska, 2001). Hydrogen adsorption on reduced mixed oxides had already been reported on $CeM_{0.5}Ni_xO_y$ and Cu added Fe/Ce/Zr mixed oxides were investigated by Jalowiecki et al. (2008) and Hong-Soon et al. (2010) through experimentation at high temperatures. In the gas phase, hydrogen readily attaches to other molecules or atoms. The molecular cations H_2^+ and H_3^+ have only a transitory existence in the gas phase. Metal oxides are surrounded by H_2 resulting in an instantaneous polarity on the atom. During this time, the polarized atom acts as a very weak dipole. The molecular form of H_2 binds with the oxide surface under ambient conditions induced by Van der Waals forces (meV range). A few studies have been reported regarding hydrogen adsorption on reduced (H_2 reduction) oxides/mixed oxides and magnesium containing alloys (milled mixture) (Cui et al., 1996). A full feature of hydrogen sorption study in reduced mixed oxide at ambient conditions and characterizations of mixed oxide and hydrogen adsorbed reduced mixed oxides are essential to realize its applications as energy storing material.

In this work, we studied the hydrogen sorption capacity of reduced mixed oxides and it hydrogen adsorption thermodynamics, kinetics at a near ambient conditions, and activation energy of desorption. Different techniques have been used to explore the mixed oxides and hydrogen adsorbed reduced mixed oxides properties as hydrogen adsorbents.

2. Experimentation

2.1. Adsorbent preparation

The hydrotalcite derived mixed oxides containing magnesium, nickel and aluminium (MNAM) were synthesized by using the coprecipitation method (Salam et al., 2013a, 2013b) from metal nitrate precursors and Na_2CO_3 as the precipitating agent. Three solutions, each containing appropriate quantities of the metal nitrate precursors of magnesium, nickel, and aluminium were prepared. The mixed nitrate solution was added drop wise into a 0.5 M sodium carbonate solution maintained the temperature 55 °C with a vigorous stirring to get the optimum precipitate of layered material. The pH was varied from 12.5 to 9. The resulting precipitates were washed several times to remove the excess Na^+ and NO_3^- ions then filtered and dried. The fresh dried material was calcined at 650 °C for 2 h to convert the mixed oxides. The mixed oxides samples were designated by MNAM-xyz, respectively; MNAM stands for Mg–Ni–Al mixed oxides and xyz stands for the molar ratios of the Mg:Ni:Al samples.

2.2. Experimentation

An elemental chemical analysis for magnesium, cobalt and aluminium has been performed using the ICP-MS (Inductively coupled plasma mass spectrometry), from Agilent 7500 series. Mixed oxides identification and its crystallinity were analysed by using powder X-ray diffraction (XRD) technique using a Bruker D8 advanced diffractometer with Cu Kα radiation. The surface morphology of the mixed oxides were studied by using a field-emission scanning electron microscope (FESEM) from the CARL Zeiss Supra 55VP instrument equipped with the Oxford INCA 400 EDX microanalysis system. The characterization of microstructure (specially SAED pattern) of mixed oxides has been carried out using a CARL Zeiss LIBRA^R 200FE transmission electron microscope with an acceleration voltage of 200 kV on ultrasonically dispersed samples in isopropanol. Nitrogen gas adsorption–desorption isotherms of the samples were obtained using a micromeritics ASAP 2020 sorptometer. The total surface areas (S_{BET}) were calculated with the Brunauer–Emmet–Teller (BET) method.

The hydrogen adsorption equilibrium and the kinetics on the mixed oxides at a near ambient temperatures and pressure were measured using a micromeritics ASAP 2020C chemical adsorption apparatus. The pretreatment of the adsorbents performed as a temperature programme reduction (TPR) procedure (A 20 mg sample was reduced by a 5% H_2 gas balanced with N_2 gas flowing at 20 ml/min and, with the heating rate of 10 °C/min up to 850 °C than cool down to 30 °C before hydrogen adsorption isotherm analysis at 30 °C and a pressure ranging from 0 to 760 mmHg. High purity hydrogen gas (99.999%) was introduced into a separate gas inlet of the adsorption unit for the hydrogen adsorption measurements. Two more adsorption isotherms of MNAM-211 have been performed at 60 °C and 90 °C to calculate thermodynamics of hydrogen adsorption using same method. The final adsorbed amount at the terminal pressure gave the adsorption equilibrium amount at a certain condition. H_2-TPD have been carried out following the TPR experiments after cooling the reduced sample to 30 °C by using a Thermo Finnigan TPD/R/O 1100 instrument. The samples were maintained at 30 °C under a flow of hydrogen to adsorb hydrogen using the same analysis method that was conducted for the hydrogen adsorption by using ASAP 2020 C. The H_2-TPD was conducted up to the temperature of 500 °C with a ramp of temperature of 5 °C/min and under the flow of nitrogen 20 ml/min. A gas calibration for the 5% H_2 in N_2 (20 ml/min) was performed to determine the TCD signal response. TCD responses represent the different concentration of H_2 and quantify the peak area to the volume data of H_2-TPD using calibration factor and sample amount. Two more H_2-TPD of MNAM-211 has been conducted at different heating rates (7 °C/min and 9 °C/min) to calculate desorption activation energy.

The Raman spectra of hydrogen adsorbed mixed oxides MNAM-211 powder was analysed by a HORIVBA Jobin Yvon, HR800 spectroscopy equipped with micro-raman set up and 'NGSLabspec' computer programme. The FTIR spectra of hydrogen adsorbed mixed oxide of MNAM-211 were recorded using Perkin Elmer Spectrum One FTIR spectrometer with

Please cite this article in press as: Salam, M.A., et al., Catalytic hydrogen adsorption of nano-crystalline hydrotalcite derived mixed oxides. Chem. Eng. Res. Des. (2013), http://dx.doi.org/10.1016/j.cherd.2013.05.024

Table 1 – Elemental composition and textural properties of MNAM with different molar ratios.

Adsorbent name	M^{II}/M^{III} (expt.)	Elemental composition			BET surface area/(m^2/g)
		Mg	Ni	Al	
MNAM-031	3.25	–	18.89	5.81	110
MNAM-121	2.94	4.75	7.62	4.20	284
MNAM-211	3.07	9.38	5.02	4.69	325
MNAM-301	2.92	17	–	5.81	124

auto image microscope attachment in the frequency region of 100–5000 cm^{-1}. The surface composition of the hydrogen adsorbed reduced mixed oxide of MNAM-211 was determined by X-ray photoelectron spectroscopy (XPS) using a Perkin Elmer 1257 model, operating at a base pressure of 3.5×10^{-6} Pa at 300 K with a non-monochromatized Al Kα line at 1486.6 eV and a hemispherical sector analyser.

3. Results and discussion

3.1. *Adsorbents physiochemical properties*

The elemental chemical analysis using ICP-MS is summarized in Table 1 where the results are shown in metal weight percent. The molar ratios of the metal in the mixed oxides are close to the value in the starting solutions (synthesis molar ratio). The results demonstrate that the degrees of the precipitation of the metals are about 95%, and the mixed oxides are homogenous.

Hydrotalcite decomposition can be performed through a few steps below such as dehydration, dehydroxylation and the decomposition of anions and resultant yields are the crystalline mixed oxides (Ping et al., 2011)

$$[M^{II}_{(1-x)}M^{III}_{x}(OH)_2](A^{n-})_{x/n} \cdot mH_2O \rightarrow [M^{II}_{(1-x)}M^{III}_{x}(OH)_2]^{x+}(A^{n-})_{x/n}$$
$$\rightarrow [M^{II}_{(1-x)}M^{III}_{x}O]^{x+}(A^{n-})_{x/n} \rightarrow M^{II}_{(1-x)}M^{III}_{x}O_{1+(x/2)}$$
$$\rightarrow M^{II}O + M^{II}M^{III}_{2}O_4 \quad (1)$$

The XRD patterns of the mixed oxides are shown in Fig. 1 indicate that the precursor of the synthesized materials have been decomposed fully at 650 °C and have led to the various oxide derivatives. The XRD analysis results compared with

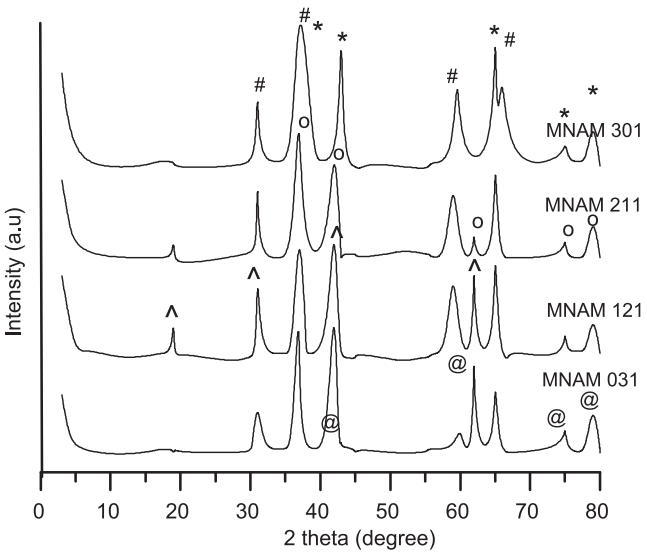

Fig. 1 – XRD pattern of MNAM mixed oxides with different molar ratios (Used symbol indicate: MgO = '*', $MgAl_2O_4$ = '#', NiO = '@', $NiAl_2O_4$ = '^', (Mg,Ni)-O = 'o').

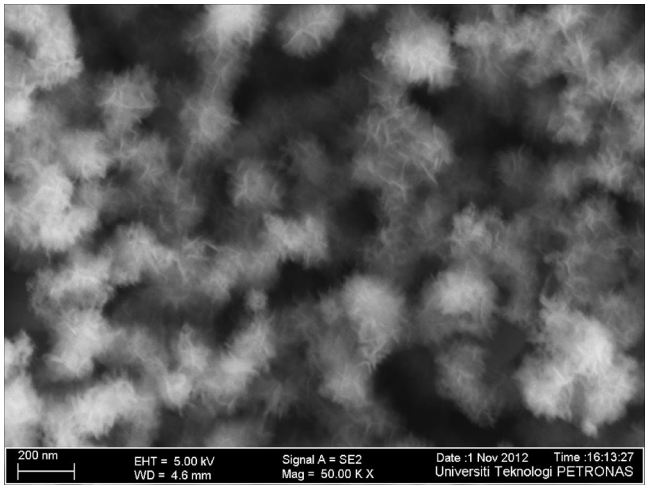

Fig. 2 – FESEM Micrograph of porous surface of MNAM-211.

the JCPDS (joint committee of powder diffraction standard) references to assign the oxides and spinels of corresponding materials. The oxides and spinels have been symbolized with different symbols in Fig. 1. For samples containing both Mg and Ni and Al, the oxides are mainly of the spinel phase with the characteristic diffraction peaks of $NiAl_2O_4$ (JCPDS 10-0339), Mg_2NiO_4 (JCPDS 1-77-396) and magnesium aluminates, $MgAl_2O4$ (JCPDS-21-1152) in addition to the individual spinels: nickel oxides, (JCPDS-22-1189) and magnesium oxides MgO (JCPDS-4-829). The situation of overlapping is also observed between MgO and some of the spinels. The elemental analysis and XRD results clearly correspond and show that the mixed oxides are homogenous and nano-crystalline. The measured crystal sizes lies in the 20–23 nm range.

The FESEM image of MNAM-211 exhibits a porous microstructure (Fig. 2) which can be ensured by BET nitrogen adsorption–desorption at −196 °C. The surface morphology of the mixed oxides depends on the synthesis condition (temperature, pH) and chemical composition. The mixed oxides show two types of morphology which are the hexagonal plate-like with an opening pore (not shown here) and the coral-like (MNAM-121) with a pore size of 80–100 nm and a slit-shape pore between two plates. Porous materials with plate-like particles have geometry with openings between the plates.

The nitrogen adsorption–desorption isotherms of the Mg–Ni–Al mixed oxides with different molar ratios showed a Type IV isotherm which indicates that the investigated materials are mesoporous. The slit-like pore allowed the adsorption of the H_2 molecule with the nearest neighbour interactions. Mixed oxides with different molar ratios exhibited quite a narrow pore size distribution (PSD). The narrow pore size distribution curve (not shown here) implied that this material possessed very regular pore channels. The textural properties obtained from the BET analysis are summarized in Table 1.

The temperature programmed reduction (TPR) results (Fig. 3) ensured that most of the mixed oxides reduced

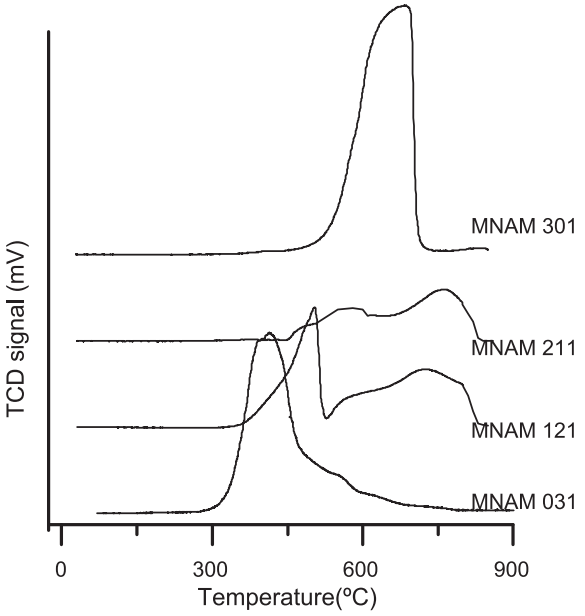

Fig. 3 – TPR profile of Mg–Ni–Al mixed oxides with different molar ratios.

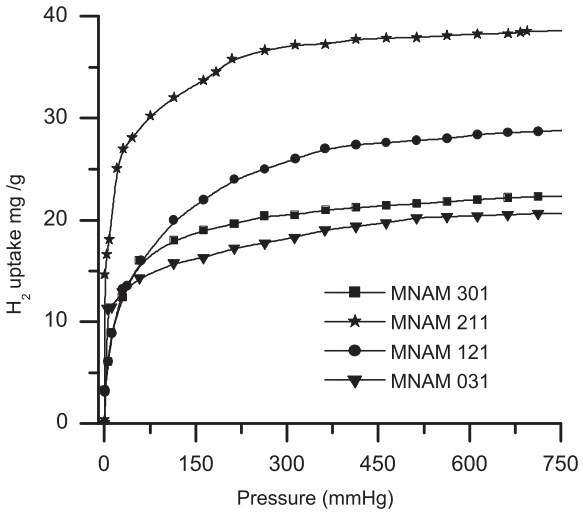

Fig. 4 – Hydrogen adsorption capacity of reduced MNAM with different molar ratios.

and activated for hydrogen adsorption. The reductions phenomena have been classified below. One reduction peak with a higher intensity is observed at 410 °C for binary mixed oxides of MNAM-031 and the peak reached to the base line with a shoulder. Aluminium supported NiO showed its reduction peak at 410 °C which can be ascribed to the reduction of Ni^{2+} species from NiO present (Rives et al., 1995) in the mixed oxides whereas the reduction of unsupported NiO is known to display a single reduction peak at approximately 367 °C (in the range of 250–427 °C).

$$NiO + H_2 \leftrightarrow Ni^o + H_2O$$

Thus, the peak indicates to the NiO reduction since this peak cannot be seen in the reduction profile of MNAM-301. Meanwhile, The longer soldier with wide range of temperature is might be due to the reduction of remaining Ni^{2+} species in Ni(Al)O ($NiO{\cdot}Al_2O_3 \rightarrow Ni^o/Al^o$) that showed subsequent hydrogen uptake as temperature is decreased which was evidenced by tailing of the curve.

The TPR profile of MNAM-301 indicates a peak maximum at 675 °C which is due to the reduction of Mg from the free MgO phase as equation below. Only one reduction peak present in the mixed oxides at higher temperatures may be due to the absence of isolated MgO in the Mg(Al)O solid solution (Dung et al., 1998)

$$MgO + H_2 \leftrightarrow Mg^o + H_2O$$

The ternary mixed oxides, MNAM-121 and MNAM-211, show different reduction patterns from those of binary oxides. The mixed oxide of MNAM-211 showed two reduction peaks. The reduction of nickel oxide (NiO) at 510 °C which is due to the weak interaction between NiO and the Mg(Al)O phase.

The increase in the nickel (molar ratio) enhanced a weakening of this interaction which lowers the reduction temperatures. The less content of nickel decrease the reducibility of NiO and increase of magnesium (molar ratio) in the Mg(NiAl)O solid solution make the peak less intense and reduction occurred in a wide range of temperature (450–850 °C). It can be seen from TPR profile of MNAM-121 and MNAM-211 (Fig. 3), when the Mg content is increased in the MNAM-211 mixed oxides, the reduction peaks shifted towards higher temperature. The higher reduction temperature for higher magnesium (Mg) molar ratio which is due to the stabilization of the Ni^{2+} that is incorporated into the periclase Mg(Al)O via the formation of solid solutions such as Mg(Ni,Al)O (Rives et al., 1995). In this case, the nickel (Ni) react with the MgO yielded NiO–MgO solid solution which is highly stable and difficult to be reduced. It is worth mentioning that the solid solution of Mg(NiAl)O melt down if the reduction temperature goes higher than 850 °C. The increase of NiO reduction temperature for ternary mixed oxides (Mg(NiAl)O solid solution) than that of binary mixed oxides attributed that homogeneous inter-dispersion of the elements in mixed oxides yielded a strong interaction among them in the correspondent mixed oxides.

The second broad peak with maxima at 750 °C temperature can be assigned to the reduction of the non-stiochiometric amorphous nickel aluminate or nickel oxides strongly interacted with the Mg(Al)O phase (Ichikuni et al., 2000).

$$Ni_xAl_2O_{3+x} + x{\cdot}H_2 \leftrightarrow x{\cdot}Ni^o + x{\cdot}H_2O + Al_2O_3$$

The ternary mixed oxide is better than the binary mixed oxides for hydrogen adsorption since the multi-composition reduced elements catalyse each other to reduce fully and create better surface for adsorption.

3.2. *Hydrogen sorption of mixed oxides adsorbent*

The hydrogen adsorption capacities of the Mg–Ni–Al reduced mixed oxides are shown in Fig. 4. MNAM-031 or mixed oxides without magnesium show less hydrogen adsorption capacity whereas MNAM-301 or mixed oxides without nickel achieved higher capacity than that of MNAM-031. The trend of the results is consistent with the stiochiometric capacity of magnesium and nickel. The significant phenomenon that can be observed, ternary mixed oxides show higher hydrogen adsorption capacities than binary mixed oxides (Table 2). MNAM-211 shows 3.9 wt% hydrogen adsorption capacity. Nickel works as a co-factor to improve kinetics, lower the binding energies of hydrogen with a magnesium surface and reduced the migration barrier for the hydrogen, thus enhancing fast loading and uploading of hydrogen. The surface of reduced mixed oxides has a different lattice structure than a pure element structure (Mg) which is also an important factor to enhance the

Please cite this article in press as: Salam, M.A., et al., Catalytic hydrogen adsorption of nano-crystalline hydrotalcite derived mixed oxides. Chem. Eng. Res. Des. (2013), http://dx.doi.org/10.1016/j.cherd.2013.05.024

Table 2 – Hydrogen adsorption and desorption capacity of reduced mixed of MNAM.

Adsorbent	Ads. capacity/(mg/g adsorbent)	Des. capacity/(mg/g adsorbent)
MNAM-031	20.40	4.98
MNAM-121	28.80	15.72
MNAM-211	38.69	18.95
MNAM-301	22.40	5.75

sorption of hydrogen. The dissociation of hydrogen molecules on the surface might occur with the help of nickel (Huang et al., 2006). Magnesium with other light, main group elements such as aluminium (Al) lowers the affinity to hydrogen and competes with hydrogen for the valance electron of magnesium (Topler et al., 1982), and reduces the bonding strength between magnesium and hydrogen. Though nickel catalyses the magnesium to enhance the hydrogen adsorption, it reduces the weight percent of hydrogen in hydride. A mechanism can be considered for hydrogen adsorption on the basis of investigated chemical and structural properties. The dissociated hydrogen penetrates into magnesium and rapidly forms a layer of MgH_2 due to the negligible solid solubility of the hydrogen in the magnesium which also prevents the hydrogen for further diffusion. In the binary and ternary reduced mixed oxide, hydrogen may diffuse along boundaries between the Mg_2Ni and Mg_3Al_2 phases and also inside the Mg_2Ni phase. The hydrogen bonded with different phases of the magnesium compound and the resultant yields (Duarte et al., 2006; Billur et al., 2007) below can be observed through the characterizations performed in this study:

$$Mg + nH = MgH_n,$$

$$Mg_2Ni + nH = Mg_2NiH_n$$

3.3. *Sorption thermodynamics and kinetics*

According to the investigation, a majority of the total chemisorption occurs in the isotherm pressure range of 40–80 mmHg. The temperature dependant adsorptions lie in this pressure range. The van't Hoff equation is an efficient tool to observe the pressure–temperature relationship of hydrogen adsorption.

$$\ln(P) = \frac{\Delta H}{RT} - \frac{\Delta S}{R} \quad (2)$$

where, ΔH is the enthalpy of the hydride in kJ/mol and ΔS is the entropy change in kJ/mol k, R is the gas constant = 8.314 J/k mol, P is the mean pressure of isotherm. A plot of ln(P) verses 1/T shown in Fig. 5 which gives the adsorption entropy (ΔS_{ads}) and enthalpy change (ΔH_{ads}) of 120.56 J/mol k and 47.25 kJ/mol, respectively. The thermodynamics values are more promising compare to the previous investigation (Yamada et al., 2001; Noritake et al., 2002) due to the reduced mixed oxides of magnesium containing nickel and aluminium. The enthalpy value predicted that the adsorption was chemisorption dominant since the chemisorptions enthalpy range is in between 40 and 120 kJ/mol. The results attributed that the adsorption process was exothermic and favourable for high temperatures since reduced mixed oxides reacted with hydrogen with different conditions and were catalysed by nickel (Lin and Chen, 2004). The negative value of the entropy indicated the randomness of the hydrogen

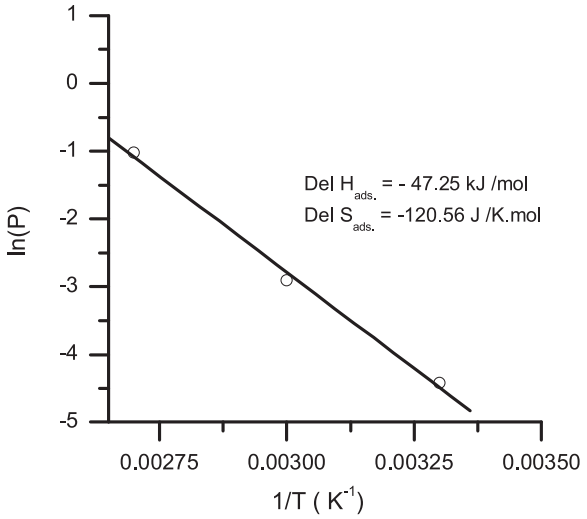

Fig. 5 – Van't Hoff plot of MNAM system.

decreased from the molecular state to the adsorbed state and the regular ordering of the hydrogen on the mixed oxides surface.

Hydrogen adsorption kinetics can be assumed by observing the type I adsorption isotherm (Fig. 4) curves. The maximum hydrogen adsorbed in the pressure range of 40–80 mmHg which is indicated that the phenomena were fast (based on time). The freshly reduced mixed oxides were in the activated form and ready to adsorb hydrogen physically and chemically. Dissociated hydrogen diffused to bulk and reacted with active site of the metal surface and adsorbed into the pores. This is the reason for showing fast hydrogen adsorption kinetics.

H_2-TPD profile of ternary mixed oxide displayed two significant desorption peaks (Fig. 6). The first peak at around >200 °C which is due to the desorption of hydrogen from Mg_2NiH_4 and the second peak around 350–400 °C is due to the hydrogen desorption from MgH_2. Hydrogen adsorbed phases of MgH_2 and Mg_2NiH_4 generally decompose at the temperature range of 200–400 °C and follow the decomposition reaction as mentioned below (Zou et al., 2012)

$$Mg_2NiH_4 \rightarrow Mg_2Ni + 2H_2 (240^\circ C)$$

$$MgH_2 \rightarrow Mg + H_2 (395^\circ C)$$

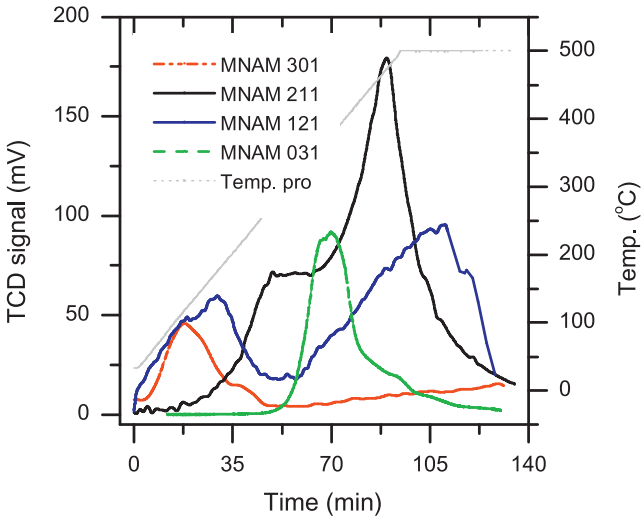

Fig. 6 – H_2-TPD of mixed oxides of MNAM with different molar ratios.

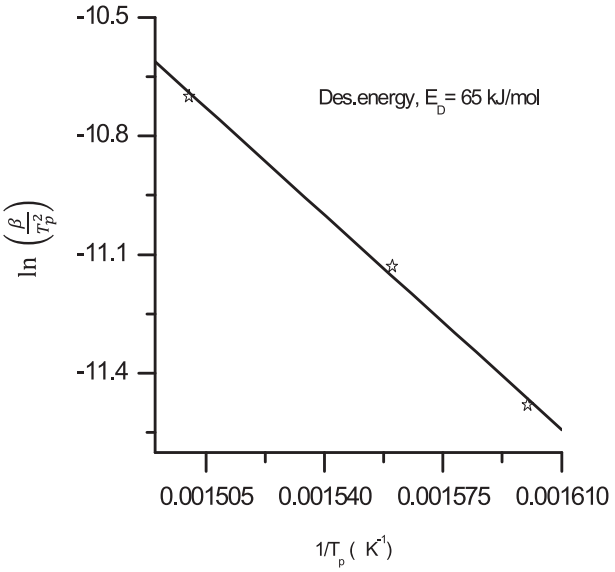

Fig. 7 – Desorption activation energy of MNAM-211.

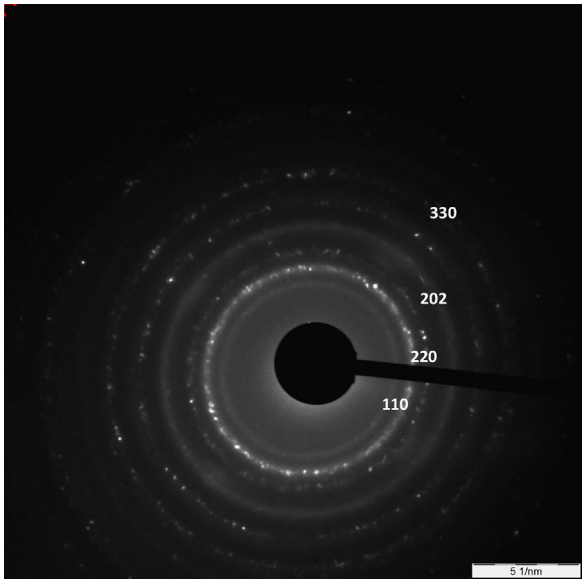

Fig. 8 – SAED pattern of hydrogen adsorbed crystal of MNAM-211.

So, the maximum hydrogen was desorbed from the mentioned hydrogen adsorbed phases as showed above. The metal-support interaction showed an important role. During desorption, hydrogen atoms on the support would migrate back to the metal surface and recombine with hydrogen molecules then desorb from the surface due to the hydrogen spillover process between them. It is thought that the electronic property of Ni^{o} changes more rigorously with increasing the molar content of Mg and Ni (Kim et al., 2005) which enhance the adsorption and desorption process.

The activation energy of desorption mainly predicts the energy that is needed to desorb hydrogen from hydrogen adsorbed materials. With the corrected kinetic equation suggested by Kissinger's following the relation between the heating rate and active gas molecules, activation energy can be calculated using the equation below:

$$ln\left(\frac{\beta}{T_p^2}\right) = \ln\frac{AR}{E_d} - \frac{E_d}{RTp} \quad (3)$$

where, T_p is the desorption peak temperature (K), β is the heating rate (K/min.) E_d is the energy of desorption is in kJ/mol, A is the pre-exponential factor (1/sec). The slop value of a plot of $\ln(\beta/T_p^2)$ verses $1/T_p$ is used to calculate the energy of desorption (Fig. 7). The linear fitting of the logarithmic relation (Kissinger's equation) provides activation energy of 65 kJ/mol under a constant driving force (1 bar). So, the calculated activation energy and thermodynamics may consider for thermal dissociation of hydrogen across the metal–hydrogen interface.

3.4. *Hydrogen adsorbed phase characterizations*

The microstructures of Mg–Ni–Al mixed oxide investigated by using high resolution transmission electron microscopy (HRTEM) together with their electron diffraction pattern. The average crystal size was 12–22 nm and hexagonal plate-like (not shown here). Most of the investigated mixed oxide adsorbents as appeared in the high resolution images (HRTEM) were polycrystalline. The diffused rings and with bright spots in the SAED pattern (Fig. 8) of hydrogen adsorbed crystal of MNAM-211 indicated the planes of (1 1 0), (2 0 2), (2 2 0), and (3 3 0). The planes are corresponding that the crystal is consisted with MgH_2, Mg_2NiH_4 and MgO (Zou et al., 2012; Tanaka et al., 1999). The sample was kept under high vacuum for several hours during analysis. It is reasonable to consider that dehydration might be occurred in this period. The diffuse rings correspond the hydrogen adsorbed phases that can be confirmed through the post characterizations of hydrogen adsorbed reduced mixed oxides by using XPS, FT-IR ad Raman techniques. The nano-crystalline material has a well-established diffusion path for the hydrogen atom along the numerous grain boundaries and a slit shaped pore with opening geometry. In the case of nickel containing nano-crystalline mixed oxides, the nickel atoms may occupy meta-stable positions in the deformed grains that are caused by the change of the electronic structure of a valance band. So the strong modifications of the electronic structure of nano-crystalline mixed oxides could effectively influence their hydrogenation behaviour.

FT-IR and Raman spectra of hydrogen adsorbed MNAM-211 are shown in Fig. 9. The IR spectrum showed the three IR band at 450, 1000 and 1650 cm^{-1}. The bands at 450 and 1000 cm^{-1} are due to the formation of MgH_2 after adsorption of hydrogen (Hiroshi, 2010; Santisteban et al., 2000). And the band at 1650 cm^{-1} is attributed to the formation of Mg_2NiH_4 (Huang et al., 1989). Raman spectrum of hydrogen adsorbed MNAM-211 displayed several Raman shifts. Three Raman shifts at 313, 950 and 1270 cm^{-1} ensured the formation of the α-MgH_2 and the shifts are very consistent with the works of Santisteban et al. (2000) and Schimmel et al. (2004). Again the Raman shifts with less intensity at 509, 707 cm^{-1} attributed the formation of γ-MgH_2 (Moriwaki et al., 2006). It is not clear the Raman shift at 1600 cm^{-1}. By comparing with the FT-IR result, it can be considered that the shift is due to the Mg_2NiH_4 which indirectly implied by Nakamoto (1986).

Generally, the binding energy of elemental species is less than their corresponding hydrides because of partial extraction of one electron from the metal by the hydrogen to create the hydrides (Briggs and Seah, 1990). The spectra of Mg (1s), Mg (2p), Ni(2p) and Al (2p) are shown in Fig. 10.

Please cite this article in press as: Salam, M.A., et al., Catalytic hydrogen adsorption of nano-crystalline hydrotalcite derived mixed oxides. Chem. Eng. Res. Des. (2013), http://dx.doi.org/10.1016/j.cherd.2013.05.024

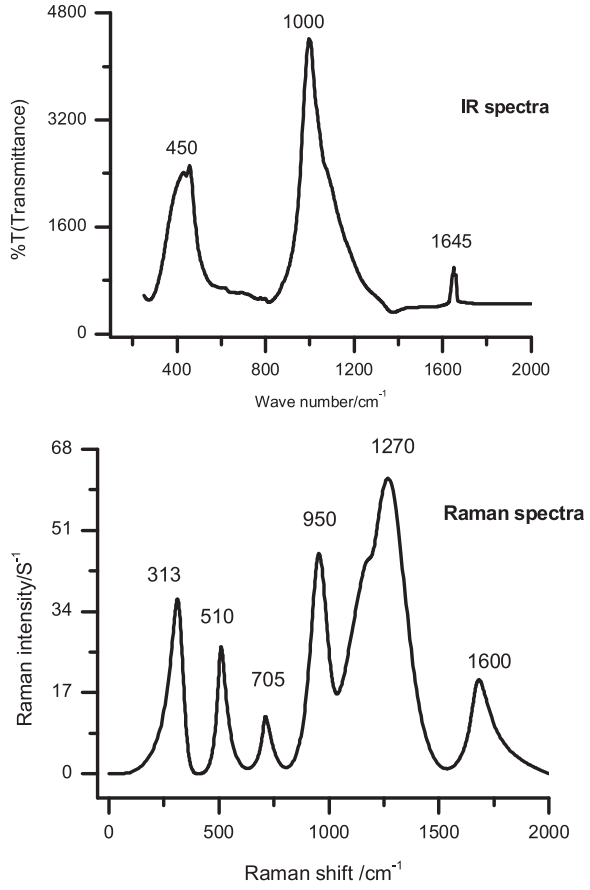

Fig. 9 – FT-IR (top) and Raman (bottom) spectra of hydrogen adsorbed MNAM-211.

It can observe that the compound, MgH_2 and Mg_2NiH_4 are formed after hydrogen adsorption which consisted with those species in where the hydrogen could be realized with the increased binding energy of the corresponding species. The nano-crystalline magnesium noticed two components that are at 49.6 and 51.8 eV indicating to metallic and oxidized magnesium species, respectively (Friedrichs et al., 2007). The state of O (1s) peak at 533.2 eV (not shown) corresponds the water or hydroxide adsorbed on the surface of magnesium particles. Reduced metal oxides absorbed hydrogen and form above mentioned hydrogen adsorbed phases. The surface adsorbed hydroxides/water from vacuum during analysis and open environment. After hydrogenation the peak of the Mg 1s and Mg 2p become broad due the overlapping of the different Mg containing compound (oxides, hydroxides and hydrides) with closer binding energies to each other (Friedrichs et al., 2006). Again, the reported peaks at 1305.3 eV and 1303.5 eV are for the oxidized state and metallic state of magnesium (Mittal et al., 2004). The peak binding energy range is 1303–1308 eV for Mg (1s) level attributes the formation of different magnesium containing compounds as well. Moreover, the peak position of the Ni (2p) reveals that nickel is in metallic state. So, it can be realized that the metallic behaviour of the Mg_2NiH_4. The compound of mixed species modified its electronic structure of polycrystalline Mg_2NiH_4 ternary hydride phase which influence the hydrogenation. The presence of Mg, Ni and Al in a compound reduce the formation of $Mg(OH)_2$ and enhance the hydrogen diffusion reactions (Anik et al., 2009). Al_2O_3 form a layer on the surface to retarding oxidation reactions but it reduces the life cycle of adsorbent.

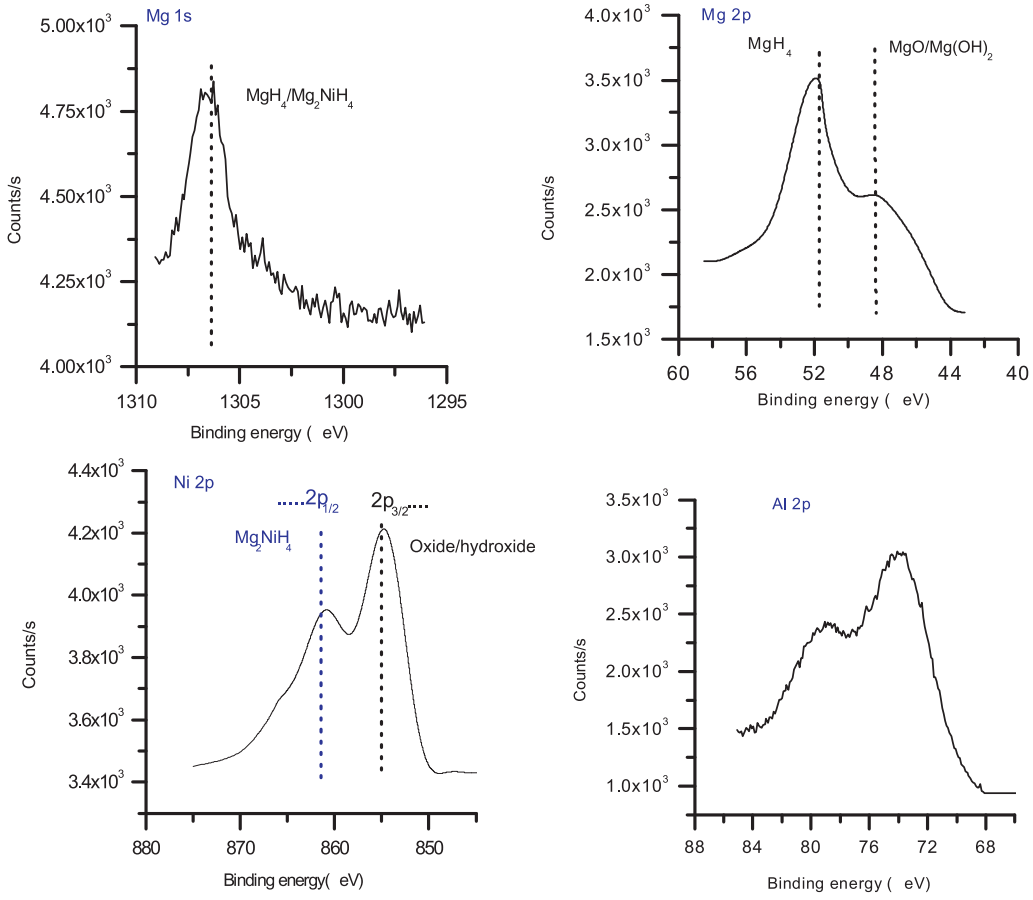

Fig. 10 – XPS spectra of Mg 1s, Mg 2p, Al 2p and Ni 2p of the hydrogen adsorbed reduced solid solution of MNAM-211.

Please cite this article in press as: Salam, M.A., et al., Catalytic hydrogen adsorption of nano-crystalline hydrotalcite derived mixed oxides. Chem. Eng. Res. Des. (2013), http://dx.doi.org/10.1016/j.cherd.2013.05.024

4. Conclusion

The mixed oxides and hydrogen adsorbed mixed oxides have been characterized using different techniques to investigate the hydrogen sorption physio-chemical properties at near ambient condition. Nickel catalysed and enhanced the adsorption and desorption process at the ambient temperature (30 °C) and pressure (760 mmHg) and the nano-level polycrystalline reduced mixed oxides of MNAM-211 showed a 3.9 wt% hydrogen adsorption capacity. The co-existence of aluminium and nickel could modify the electronic structure of the mixed oxides surface and dissociated reactive hydrogen species that diffuse and bind from bulk to different transitional phases and desorbed at 395 °C. The calculated desorption activation energy of 65 kJ/mol implied the hydrogen release behaviour of adsorbent. XPS, Raman and FTIR analysis confirmed the hydrogen adsorbed phase of MgH_2 and Mg_2NiH_4. The material can be used to different industrial application as energy carrier.

Acknowledgements

We would like to acknowledge gratefully the financial support of this research by the FRGS grant 158-200-092, Malaysia.

References

Arean, C.O., Chavan, S., Cabello, C.P., Garrone, E., Palomino, G.T., 2010. Thermodynamics of hydrogen adsorption on metal-organic frameworks. ChemPhysChem 11 (42), 3237–3242.

Anik, M., Gasan, H., Topcu, S., Akay, I., Aydinbeyli, N., 2009. Electrochemical hydrogen storage characteristics of $Mg_{1.5}Al_{0.5-x}Zr_xNi$ ($x = 0$, 0.1, 0.2, 0.3, 0.4, 0.5) alloys synthesized by mechanical alloying. Int. J. Hydrogen Energy 34, 2692–2700.

Bogdanovic, B., Hartwig, J.H., Spliethoff, B., 1993. The development, testing and optimization of energy storage materials based on the MgH_2–Mg system. Int. J. Hydrogen Energy 18, 575–589.

Borgschulte, A., Westerwaal, R.J., Rector, J.H., Schreuders, H., Dam, B., Griessen, R., 2006. Catalytic activity of noble metals promoting hydrogen uptake. J. Catal. 239, 263–271.

Bergaya, F., Theng, B.K.G., Lagaly, G., 2006. Hand Book of Clay Science, Developments in Clay Science, 1. Elsevier, Amsterdam, pp. 1224.

Billur, S., Farida, L.D., Michael, H., 2007. Metal hydride materials for solid hydrogen storage: a review. Int. J. Hydrogen Energy 32, 1121–1140.

Bergada, O., Vicente, I., Salagre, P., Cesteros, Y., Medina, F., Sueras, J.E., 2007. Microwave effect during aging on the porosity and basic properties of hydrotalcites. Microporous and Mesoporous Mater. 101, 363.

Briggs, D., Seah, M.P. (Eds.), 1990. Practical Surface Analysis. , 2nd Ed. Wiley, Chichester.

Cui, N., Luan, B., Zhao, H.J., Liu, H.K., Dou, S.X., 1996. Effects of yttrium additions on the electrode performance of magnesium-based hydrogen storage alloys. J. Alloys Compd. 233, 236–240.

Cornelis, P.B.D., Bart, P.C.H., Johannes, H.B.D., Krijn, P.J., 2006. Facilitated hydrogen storage in $NaAlH_4$ supported on carbon nanofibers. Angew Chem. Int. Ed. 45, 3501–3503.

Duarte, G., Bustamante, L.A.C., Miranda, P.E.V., 2006. Hydriding properties of a Mg–Al–Ni–Nd hydrogen storage alloy. WHEC 16, 13–16.

Dung, N.T., Tichit, D., Chichea, B.H., Coq, B., 1998. Influence of the thermal treatments of a (Ni.Mg)/Al layered double hydroxide in the hydrogenation of acetonitrile. Appl. Catal. A: Gen. 169, 179–187.

Friedrichs, O., Sanchez-Lopez, J.C., Lopez-Cartes, C., Dornheim, M., Klassen, T., Bormann, R., Fernandez, A., 2006. Chemical and microstructural study of the oxygen passivation behaviour of nanocrystalline Mg and MgH_2. Appl. Surf. Sci. 252, 2334.

Friedrichs, O., Kolodziejczyk, L., S'anchez-L'opez, L.C., L'opez-Cart'es, C., Fern'andez, A., 2007. Synthesis of nanocrystalline MgH_2 powder by gas-phase condensation and in situ hydridation: TEM XPS and XRD study. J. Alloys Compd. 434/435, 721–724.

Hiroshi, H., 2010. Quantitative evaluation of catalytic effect on the desorption reaction of hydrogen storage materials on the basis of atomization energy concept. Nagoya University (PhD thesis).

Hong-Soon, K., Kwang-Seo, C., Byoung-Kwan, Y., Tae-Gong, R., Young-Seak, L., Chu-Sik, P., Young-Ho, K., 2010. Chemical hydrogen storage and release properties using redox reaction over the Cu-added Fe/Ce/Zr mixed oxide medium. J. Ind. Eng. Chem. 16 (1), 81–86.

Huang, N., Yamauchi, H., Wu, J., Wang, Q.Z., 1989. Switchable mirrors based on nickel magnesium films. Phys. Chem. Munich 163, 225.

Huang, L.J., Liang, G.Y., Sun, Z.B., Wu, D.C., 2006. Electrode properties of melt-spun Mg–Ni–Nd amorphous alloys. J. Power Sources 160, 684–687.

Ichikuni, N., Murata, D., Shimazu, S., 2000. Promoting effect of $NiAl_2O_4$ for supported Ni particles on sprayed Ni/Al_2O_3 catalysts. Catal. Lett. 69, 33–36.

Jalowiecki, D.L., Debeusscher, S., Zarrou, H., D'Huysser, A., Jobic, H., Payen, E., 2008. Hydrogen storage in $CeM_{0.5}Ni_XO_Y$(M = Zr or Al) mixed oxides. Catal. Today 138, 266–271.

Kirm, I., Medina, F., Rodrıguez, X., Cesteros, Y., Salagre, P., Suieras, J., 2004. Epoxidation of styrene with hydrogen peroxide using hydrotalcites as heterogeneous catalysts. Appl. Catal. A: Gen. 272, 175.

Kim, P., Kim, Y., Kim, H., Song, I.K., Yi, J., 2005. Preparation, characterization, and catalytic activity of NiMg catalysts supported on mesoporous alumina for hydrodechlorination of o-dichlorobenzene. J. Mol. Catal. A: Chem. 231, 247–254.

Lin, H.Y., Chen, Y.W., 2004. The kinetics of H_2 adsorption on supported ruthenium catalysts. Thermo. Acta 419, 283–290.

Moriwaki, T., Akahama, Y., Kawamura, H., Nakano, S., Takemura, K., 2006. Structural phase transition of rutile-type MgH_2 at high pressure. J. Phys. Soc. Jpn. 75 (7), 074603.

Mittal, V.K., Bera, S., Nithya, R., Srinivasan, M.P., Velmurugan, M.P., Narasimhan, S.V., 2004. Solid state synthesis of Mg–Ni ferrite and characterization by XRD and XPS. J. Nucl. Mater. 335, 302–310.

Mahasweta, N., Mohona, S., Krishanu, S., Asim, B., 2009. 3D-hexagonal mesoporous silica having exceptional H_2 adsorption capacity. J. Phys. Chem. C 113, 6839–6844.

Nakamoto, K., 1986. Infrared and Raman Spectra of Inorganic and Coordination Compounds, 4th Ed. Wiley, New York, pp. 130–131.

Noritake, T., Aoki, M., Towata, S., Seno, Y., Hirose, Y., Nishibori, E., Takata, M., Sakata, M., 2002. Chemical bonding of hydrogen in MgH_2. App. Phys. Lett. 81, 2008–2010.

Ping, X.Z., Zhang, J., Adebajo, M.O., Zhang, H., Zhou, C., 2011. Catalytic applications of layered double hydroxides and derivatives. Appl. Clay Sci. 53 (2), 139–150.

Rives, V., Ulibarri, M.A., Montero, A., 1995. Application of temperature-programmed reduction to the characterization of anionic clays. Appl. Clay Sci. 10, 83–93.

Schimmel, H.G., Johnson, M.R., Kearley, G.J., Ramirez-Cuesta, A.J., Huot, J., Mulder, F.M., 2004. The vibrational spectrum of magnesium hydride from inelastic neutron scattering and density functional theory. Mater. Sci. Eng. B108, 38–41.

Salam, M.A., Suriati, S., Murugasen, T., 2013a. Hydrogen storage of a fixed bed of nano-crystalline mixed oxides. ISRN Nanomater., 1–10 (article ID 539534).

Salam, M.A., Lwin, Y., Suriati, S., 2013b. Synthesis of nano-structured Ni–Co–Al hydrotalcites and derived mixed oxides. Adv. Mat. Res. 626, 173–177.

Please cite this article in press as: Salam, M.A., et al., Catalytic hydrogen adsorption of nano-crystalline hydrotalcite derived mixed oxides. Chem. Eng. Res. Des. (2013), http://dx.doi.org/10.1016/j.cherd.2013.05.024

Salam, M.A., Suriati, S., Lwin, Y., 2013. Hydrogen adsorption study on mixed oxides using the density functional theory. J. Phys. Chem. Solids 74 (4), 558–564.

Shouli, B., Dianqinga, L., Dongmei, H., Ruixian, L., Aifan, C., Liu, C., 2010. Preparation, characterization of WO_3–SnO_2 nanocomposites and their sensing properties for NO_2. Sens. Actuat. B 150, 749–755.

Santisteban, J.R., Cuello, G.J., Davidowski, J., Fainstein, A., Peretti, H.A., Ivanov, A., Bermejo, F.J., 2000. Vibrational spectrum of magnesium hydride. Phys. Rev. B 62, 37.

Tanaka, K., Kanda, Y., Furuhashi, M., Saito, K., Kuroda, K., Saka, H., 1999. Improvement of hydrogen storage properties of melt-spun Mg–Ni–RE alloys by nanocrystallization. J. Alloys Compd. 293, 521.

Topler, J., Buchner, H., Aufferer, H.S., Knorr, K., Prandl, W., 1982. Measurements of the diffusion of hydrogen atoms in magnesium and Mg_2Ni by neutron scattering. J. Less Common Met. 88, 397–404.

Vajo, J.J., Olson, G.L., 2007. Hydrogen storage in destabilized chemical systems. Scripta Mater. 56, 829–834.

Yamada, T., Yin, J., Tanaka, K., 2001. Hydrogen storage properties and phase structures of Mg-rich Mg–Pd, Mg–Nd and Mg–Pd–Nd alloys. Mater. Trans. 42, 2415–2421.

Zou, J., Sun, H., Zeng, X., Ji, G., Ding, W., 2012. Preparation and hydrogen storage properties of Mg-rich Mg–Ni ultrafine particles. J. Nanomater., 1–8.

Zakrzewska, K., 2001. Mixed oxides as gas sensors. Thin Solid Films 391, 229–238.

Please cite this article in press as: Salam, M.A., et al., Catalytic hydrogen adsorption of nano-crystalline hydrotalcite derived mixed oxides. Chem. Eng. Res. Des. (2013), http://dx.doi.org/10.1016/j.cherd.2013.05.024